STATUS OF THE TAOS PROJECT AND A SIMULATOR FOR TNO OCCULTATION

Sun-Kun King[1], Charles Alcock[2], Tim Axelrod[3], Federica B. Bianco[4,2], Yong-Ik Byun[5], Wen-Ping Chen[6], Kem H. Cook[7], Yung-Hsin Chang[6], Rahul Dave[4], Joseph Giammarco[4], Typhoon Lee[1], Matthew Lehner[2,4], Jack Lissauer[8], Stuart Marshall[9], Soumen Mondal[6], Imke de Pater[10], Rodin Porrata[6], John Rice[10], Megan E. Schwamb[4], Andrew Wang[1], Shiang-Yu Wang[1], Chih-Yi Wen[1] and Zhi-Wei Zhang[6]

[1]*Institute of Astronomy & Astrophysics, Academia Sinica, Taiwan, ROC*
[2]*Harvard-Smithsonian Center for Astrophysics, Cambridge, MA, USA*
[3]*Steward Observatory, The University of Arizona, Tucson, AZ, USA*
[4]*Department of Physics and Astronomy, University of Pennsylvania, PA, USA*
[5]*Department of Astronomy, Yonsei University, Seoul, South Korea*
[6]*Institute of Astronomy, National Central University, Chung-Li, Taiwan, ROC*
[7]*Lawrence Livermore National Laboratory, Livermore, CA, USA*
[8]*NASA, Ames Research Center, Mountain View, CA, USA*
[9]*Stanford Linear Accelerator Center, Stanford, CA, USA*
[10]*University of California, Berkeley, CA, USA*
E-mail: skking@asiaa.sinica.edu.tw

The majority of trans-Neptunian objects (TNOs) are probably small comets beyond the orbit of Neptune. A study of TNOs may enable a better understanding of the origin of short-period comets and of the process of planet formation and the early history of the solar system. An occultation survey is currently the only way to detect these objects down to a size of a few kilometers at such a distance. The status of the TAOS (Taiwan-America Occultation Survey) project is reported. In order to monitor thousands of stars on the order of a fraction of a second using CCD cameras, a novel CCD readout technique, the "shutterless zipper mode", is applied. Two predicted asteroid occultation events were successfully observed. Instead of a simple number count of occultation events, an interpretation of a TNO occultation survey result can be obtained by using the simulator described here. Through comparison of the results from an observation and from our simulator, a specific astronomical or astrophysical model can be constrained.

1. Introduction

It has long been suspected that short-period comets might have a different origin than those of long-periods.[1,2] The existence of this Edgeworth-Kuiper belt was not realized until the discovery of the first (other than Pluto and Charon) trans-Neptunian object (TNO) 1992 QB_1 by Jewitt and Luu.[3] Currently, more than a thousand of them have been detected. Some of them are even compatible in size with Pluto.[4] The discovery of Sedna[5] with a perihelion around 76 AU might indicate the existence of a whole new family of TNOs in the outer solar system where the gravitation of Neptune plays a less significant role. However, the distribution of comet-size (a few kilometers) objects is still poorly-known. Preliminary results from recent observation[6] and simulation[7] show the possibility of a broken power law in the TNO size distribution. Some physical properties can be derived for the largest TNOs, but certain properties like albedo would be pure speculation and extrapolation for such small objects. One cannot study those comets in detail until their orbits bring them closer to us, such as some of the Centaurs. On the other hand, to explain the current population of the Jupiter-family comets, which is generally believed to originate from the trans-Neptunian region, 10^9–10^{10} comets of a size around 1–10 km in 30–50 AU might be required.[6,9]

Instead of trying to detect the reflected light from those distant small objects, an occultation survey[8] could probe a comet-size TNO at a few hundred AU or even farther away. The TAOS (Taiwan-America Occultation Survey) project[10–12] has a design based on this indirect strategy. Some other, smaller in scope, surveys have been conducted in recent years,[14,15,26] though convincing statistics describing small comet occultations have yet to be obtained. However, future improvement in both ground-based and space-based experiments are expected to provide deeper insight. We briefly report the status of TAOS in Sec. 2. Related information and details are available at the TAOS website.[a] Diffraction and the angular size of a target star[11,13,14] are two major factors which determine the "detectability" of a presumed occultation event or the "visibility" of an occultation dip in a light curve. Occultation is a technique which is capable of detecting a small comet as far as the inner Oort cloud. A poor distance resolution may be obtained from the angular size of a target star and the size of the foreground TNO. Recent analysis[16] suggest that it might be possible to

[a] http://taos.asiaa.sinica.edu.tw

break the degeneracy between size and distance under certain conditions when a cylindrical symmetric solution and a center-crossing event were assumed. It is not clear whether this will still be the case with a more complete parameter space when certain photometric error or noise is considered. Starting from the theory of diffraction, an ensemble of light curves can be derived with a specific astronomical distribution and/or astrophysical model assumed. These light curves will be fed into a data pipeline for photometric analysis and efficiency test. The output of this simulator can be compared with an observational result, which will be a test against the astronomical/astrophysical model assumed earlier. Details and progress of our simulator and some additional comments on a simple geometric model are presented in Sec. 3.

2. TAOS Status and Zipper Mode Test

The objective of TAOS is to simultaneously monitor thousands of stars in a field with three or four robotic telescopes running in synchronous mode at a rate of 5 Hz (the rate can be varied). This rate corresponds to a shadow of a few kilometers in size passing through a specific site at a relative speed around 25 km/s, which is dominated by the orbital velocity of the earth itself. These four dedicated small (50 cm) telescopes have a wide field of view (1.7 by 1.7 degrees). The use of at least three telescopes is to reduce false positives below a statistically significant threshold.[17,18] While having the telescopes separated by several kilometers would have provided better resolution and the possibility to determine size and shape directly, practical considerations have lead to have all the telescopes operating at one site within a hundred meter range. Follow-up observation with a larger telescope could be helpful in telling a foreground asteroid event apart.

Instead of using a multi-object photometer[15] or fiber-optics, a high-quantum efficiency, back-illuminated CCD camera (SI-800) with 2048 $\times$ 2048 pixels[b] was installed on each telescope. Following the experience from the ROTSE project,[19] control software has been developed which can perform a sky patrol automatically. A special function which can respond to a GCN (Gamma-ray-burst Coordinates Network) alert was also integrated with the software. Given the high data rate of TAOS, each telescope might collect 20 to 30 GB of data in a clear night, a nearly real-time data pipeline is needed for processing.

[b]There are actually four more rows unmasked. Some of them have different sensitivities.

The typical readout time of our 2-channel CCD camera is around 2 seconds. To use a CCD for a 5 Hz rate survey mission, a special technique is required. The strategy we use is called shutterless "zipper" mode operation.[17,18] This technique takes advantage of the standard CCD readout process where photoelectrons have to be read out sequentially in each channel. The readout time for each row (2048 pixels) is approximately 1 ms. With some modification in both its firmware and our control software, the readout process can be "held" for, say, 200 ms (the "hold-time") after a few rows were read out. These few rows (for instance, 64 rows) of data constitutes a fundamental unit of TAOS raw data, namely, a "rowblock". All stars and sky patches in a 2048 $\times$ 2048 field will be squeezed into each rowblock (say, 2048 $\times$ 64) at the final readout. However, a star image in each rowblock might be an exposure in one of the, say, 32 cycles (32 = 2048/64). A different star in the same rowblock may come from an exposure in a different cycle. Figure 1 is a simplified version which illustrates some special features of this operation. The rowblock readout reaches a steady state after a few cycles. (It takes four cycles in Fig. 1.) In reality, stars spread across the whole field randomly as shown in Fig. 1-(e). Without an original stared image, there would be no way to recover the coordinates of a star from a rowblock. This hold-readout cycle can be continued indefinitely with the shutter left open and the telescope tracking a target field. Usually, tens of rowblocks will be stored as a single file for the convenience of data processing.

Through remote control, two predicted asteroid occultation events were recorded successfully in our zipper mode images as shown in Fig. 2 and Fig. 3. In the first event, a bright star HIP 079407 (m_V = 8.80) was occulted by an asteroid (51) Nemausa (m_V = 11.9, diameter = 150 km) at around 18:55 21st February, 2004 (UTC). The hold time of each rowblock is about 0.5 seconds in Fig. 2. A magnitude drop of about 3.5 magnitude for approximately 10 seconds was detected by the TAOS B telescope. In the second event, a bright star HIP 050535 (m_V = 8.6) was occulted by (1723) Klemola (m_V = 15.7, diameter = 31 km) at around 12:10 5th June, 2004 (UTC). The hold time is 0.25 seconds in Fig. 3. An occultation lasted for approximately one second was recorded by two telescopes simultaneously.

There are a few disadvantages to shutterless zipper mode which must be addressed. For fast data acquisition the cameras are run in shutterless zipper mode. The shutter remains open, small rowblocks (e.g. 64 rows) of the CCD are read out (readout time less than 200 ms). The CCD counts are rapidly shifted with respect to the star by the size of the rowblock.

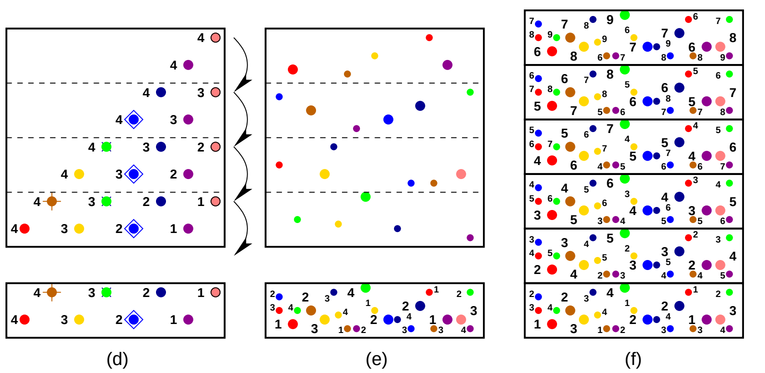

Fig. 1. Shutterless zipper mode. (a), (b), (c) and (d) illustrate the process of CCD readout under shutterless zipper mode. A square CCD chip covers a field where eight different stars happen to align across that field as shown in (a). One rowblock, which is shown right below each "CCD snapshot", is read out in each cycle. The readout direction is downward. It reaches a steady state at (d) after four cycles here while all eight different stars in this field are "squeezed" into one rowblock. Moreover, the star images in each rowblock may come from exposures in different cycles (as shown by their numerical labels). In reality, target stars spread over a field randomly as illustrated in (e). It is impossible to reconstruct a field based on its zipper image. The TAOS raw data is collected as a stack of tens of rowblocks usually. Figure 1-(f) shows what it may look like if the target field is the same one as shown in (e). But, keep in mind that as many as 32 cycles might be involved in a TAOS rowblock, which is too complicated to be shown here clearly. To move a whole rowblock downward takes time as well. Therefore, a bright star usually leaves a clear streak behind which is really exposure during the movement (not shown in the plot).

By the time a rowblock has traversed from the top of the CCD to the bottom where it is read out, it will accumulate all the stars that were in the original 2048 row image into a rowblock. Depending on sky and seeing conditions, a different size of the rowblock can be used. One downside of

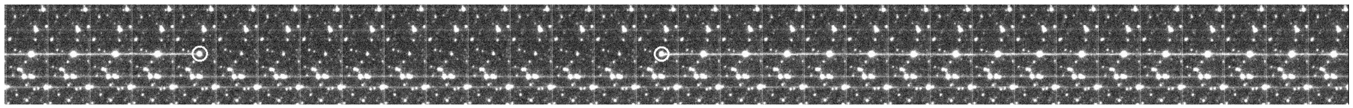

Fig. 2. Occultation of HIP 079407 by (51) Nemausa on 21st February, 2004 (UTC). Part of our raw zipper data is shown here. There are 32 rowblocks (90 degrees rotated) in this figure. Each rowblock includes 2048×64 pixels, where 151×64 pixels are shown. Each pixel corresponds to 3 arcsec in the sky. Starting from the left, each cycle lasted for about 0.5 seconds. The two circles, centered on the target star, indicate the start and the end of this occultation roughly. The asteroid itself ($m_V = 11.9$) is barely visible during occultation where the target star is missing for ten rowblocks.

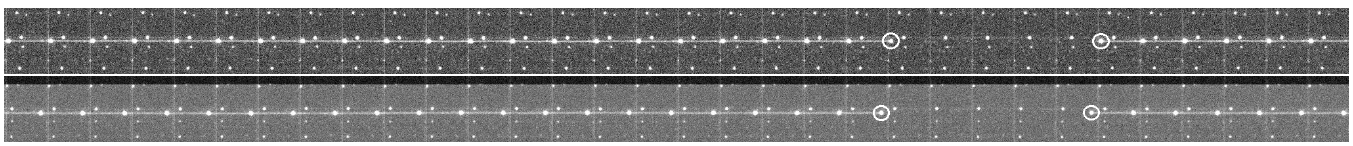

Fig. 3. Occultation of HIP 050535 by (1723) Klemola on 5th June, 2004. It is similar to Fig. 2 except that data from two telescopes A (top) and B (bottom) are shown here. Each cycle lasted for about 0.25 seconds, only. The target star HIP 050535 ($m_V = 8.6$) is clearly missing in four rowblocks between the two circles in both cases. This is the signal for an occultation lasted for about just one second. The asteroid itself is too faint ($m_V = 15.7$) to be identified during this event in our zipper image. Thirty-two rowblocks with 100×64 pixels per rowblock are shown. The two telescopes pointed at slightly different directions. Hence, stars were "zipped" into slightly different patterns.

this technique is that sky background is always collected especially during each hold-time. The sky background could be five or six times ($\sqrt{2048/64}$) brighter than that of a stared image. Because it takes a finite amount of time to read in each row of the rowblock, a small percent of each star's flux is imprinted in each row creating streaks in the image for stars brighter than 10th magnitude. This will further decrease the number of usable stars for detections. Closing the shutter during readout can remove the streak if a fast and robust shutter is available. To reduce the sky background, one will need something different. For instance, the use of a mask, a fiber system or a novel electronic design such as a multi-channel frame-transfer CCD or CMOS should have an improvement in the sky background level by one or two magnitudes.

Nevertheless, the system capability was demonstrated successfully. TAOS is supposed to conduct a "blind" occultation survey. That doesn't prevent us from observing a rare predicted event whichever might come close to the TAOS site. A local network is organized for such an event as well. Direct measurements of known Centaurs (e.g. Pholus[20]) or big TNOs[21] are possible. The light curves derived can also be used to study a variable star which varies on a larger time scale.[22] Similar techniques have been developed elsewhere independently to detect a lunar occultation event[23] and to study speckle imaging of binary stars.[24]

3. A Simulator for TNO Occultation Survey

Synchronous mode operation with three TAOS telescopes began in the winter of 2004. Reliable light curves, free from bad weather, poor seeing, lost tracking and other non-ideal conditions, are expected to be produced in large amounts. An immediate question would be, "What do the occultation survey results mean?" First of all, it is straightforward to compare the event number counts with a model prediction. The simplest model should be a geometric model where a certain solid angle is occupied by the foreground TNOs (with some kind of size and orbital distribution assumed) for a given time duration. A certain probability that a background star will be occulted can be calculated.[11,14,25,26] However, it has also been pointed out that a geometric picture may be too simple to be true because diffraction effect may increase the event rate drastically.[14] The number of TNO occultation events is dominated by the faint-end objects where, near the diffraction limit, Fresnel diffraction applies. The criterion of an occultation event is really an artificial one. An arbitrary cut-off may introduce an error which could be as big as the number count itself. Moreover, the so called "occultation event rate" depends on the system and the algorithm used. We'd say that the geometric picture is good for an estimate, but, something else is needed for an interpretation. A simulator is just what we need to understand the underlying astronomy and astrophysics.

The following steps are taken to develop the simulator. First, an ensemble of light curves are derived from a specific astronomical or astrophysical model. Next, all these light curves will be run through a specific data pipeline with a photometric algorithm applied. An efficiency test is also required here. By adding a fake signal, the efficiency of an algorithm can be obtained. The final result can now be compared with an observation to justify the model assumed. To derive an ensemble of light curves from the first principles, the physical process of TNO occultation can be simulated with the following four levels of consideration.

(1) Star level: The spectral type, luminosity class, apparent magnitude (or angular size) and, if available, a limb darkening model of a target star determine the physical properties of the diffracted light source.
(2) TNO level: The size, distance and shape of a TNO together with the astronomical or astrophysical assumption in the total population, size distribution and orbital distribution of TNOs specify the obstacle in a diffraction calculation. A diffractive shadow can be derived with the above two levels of parameters.
(3) Shadow level: Impact parameter and shadow velocity should be involved here. An occultation event doesn't have to be a center-crossing event. Nevertheless, the impact parameter can only be a random number that leads to a certain distribution. The shadow ground velocity will be coupled to the TNO distance by assuming a circular orbit. This might be a good approximation for the classical TNOs. Scattered objects have a larger dispersion in their shadow velocities.
(4) Light curve level: Filter is introduced in this level. It is proper to associate a specific term "configuration" with everything mentioned above. A configuration corresponds to the old geometric picture which relates to an ensemble of light curves with a certain probability. In addition, sampling rate and sampling phase, namely, the (random) start point of each sampling, are the last two things to be considered before an ensemble of (normalized) light curves can be derived.

The ensemble of normalized light curves will be integrated with some simulated light curves at a given flux where various kinds of noise can be added for further analysis. Photometry is the major part of the data pipeline. A preliminary photometric algorithm can be used for testing.

A few concrete examples should be helpful in understanding some of the steps above. The importance of the star level can be understood through Table 1. The limiting magnitude is around 14 in a typical TAOS zipper mode image. It is obvious that the angular size of a TAOS target star could be compatible with a comet-size TNO itself. Another interesting feature is

Table 1. Colours, magnitude, temperatures, and radius of normal stars are shown. The projection of a stellar disk at 50 AU is estimated for various apparent magnitudes (m_V) around 10 to 14. These are typical magnitudes of target stars in a TAOS zipper mode image. Some of these stellar disks are similar to a comet-size TNO in their angular sizes.

S_p	M_V	$T_{\rm eff}$	$R/R_\odot$	R (km) at 50 AU				
				$m_V = 10$	11	12	13	14
O5V	−5.7	42000	12	0.15	0.09	0.06	0.04	0.02
A0V	+0.65	9790	2.4	0.55	0.35	0.22	0.14	0.09
F5V	+3.5	6650	1.3	1.10	0.69	0.44	0.28	0.17
K0V	+5.9	5150	0.85	2.17	1.37	0.86	0.55	0.34
K5V	+7.35	4410	0.72	3.58	2.26	1.43	0.90	0.57
M0V	+8.8	3840	0.60	5.83	3.68	2.32	1.46	0.92
M5V	+12.3	3170	0.27	13.14	8.29	5.23	3.30	2.08
K0III	+0.7	4660	15	3.49	2.20	1.39	0.88	0.55
K5III	−0.2	4050	25	3.85	2.43	1.53	0.97	0.61
M0III	−0.4	3690	40	5.61	3.54	2.23	1.41	0.89

Source: "Allen's Astrophysical Quantities, 4th Edition", editor Cox, A. N., (Springer-Verlag, New York, 2000).

that Fresnel diffraction could dominate a TAOS event. Suppose a TNO is at a distance (d) of 50 AU. The related occultation is observed at a wavelength (λ) of 500 nm. The size of a TNO (s) will satisfy $s^2/(\lambda d) \sim 1$ if s is around 1 km. The code should be able to handle something like Fresnel integrals rather than just a Fourier transformation. A diffraction code was developed. It is now part of this simulator. Given all proper input parameters, a diffraction pattern and a CCD response at a certain sampling rate with various sampling phase can be derived as illustrated in Fig. 4. Only spherical TNOs of comet-size at trans-Neptunian distance are considered here. Shadow velocity, however, is a free input parameter here. It can be related to the angular separation from the opposition with a general (circular or non-circular) Keplerian orbit assumed. That velocity is a function of TNO orbital elements and the two dimensional TNO phase angle. Its

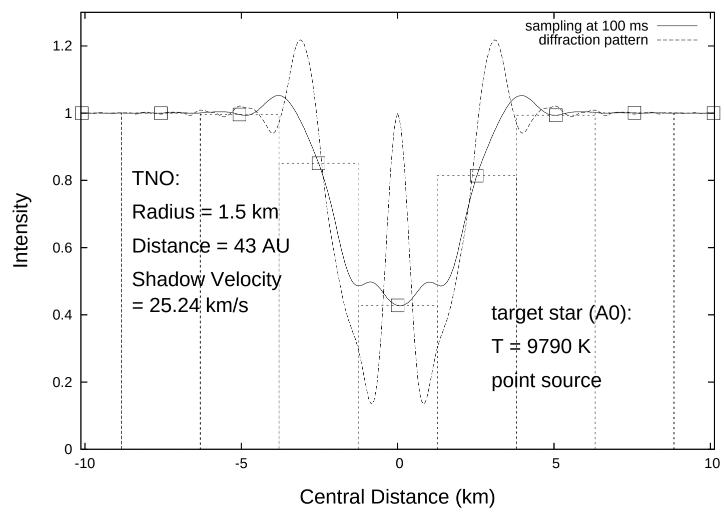

Fig. 4. Diffraction pattern and detector's response. Target star: A0 (black body at 9790 K), point source. TNO: radius 1.5 km, 43 AU away, shadow velocity 25.24 km/s. Filter: 400 to 800 nm band-pass. The diffraction pattern through the center is shown as the dash curve. Response at a sampling rate of 100 ms is shown as nine small squares. A set of light curves will fill the solid line if all possible sampling phases are considered.

dispersion can thus be related to a distribution in the orbital elements. There are some interesting relations between a random impact parameter and the distribution of geometric occultation duration. Given a spherical object with its circular shadow, this distribution can be calculated analytically. A simulation is shown in Fig. 5 (the rightmost solid line with eccentricity $e = 0$) where a target star of point source is assumed. A few more two-dimensional cases were studied. An ellipse with certain orientation is similar to a circle basically. An ellipse of certain size with random orientation has a eccentricity-dependent distribution. Its geometric occultation duration is dominated by the size of its minor axis. Figure 5 shows the cumulated probability with respect to the normalized occultation duration. (For an ellipse, it is normalized with respect to its major axis where it has the longest occultation duration.) Geometric rectangular shadows were analyzed as well. Two folding points relate to its length and its width respectively as can be seen in Fig. 5. These two points degenerate for a square shadow. However, it is not clear whether these results can be applied while diffraction is considered. By assuming theoretical distributions with enough computing power, ensembles of light curves can be generated

November 7, 2005 10:50 WSPC/Trim Size: 9in x 6in for Review Volume skking˙aogs2005

systematically. To get larger or non-spherical objects involved will require extending the existing code.

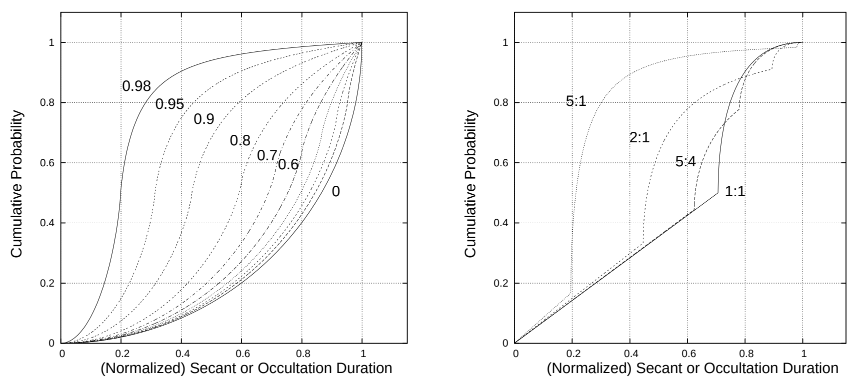

Fig. 5. Cumulative probability of the normalized geometric occultation duration for a given two-dimensional shape at a certain distance. The orientation is randomly distributed with a specific direction of shadow velocity. Target star is assumed as a point source. These are simulated results with one million events involved in each curve. The binning factor in these (cumulative) histograms is 1000. The maximum differential probabilities happen at the maximum slopes of these curves. (Left) Cumulative probability for ellipses of different eccentricities (Starting from the leftmost curve, the eccentricities are 0.98, 0.95, 0.9, 0.8, 0.7, 0.6, 0.5, 0.4, 0.3 and 0 respectively). The occultation duration is normalized with respect to its major axis. The maximum slope in each curve is associated with its minor axis. The slopes at the maximum occultation duration are related to the complete elliptic integral of the second kind. (Right) Cumulative probability for rectangles with different length to width ratios. The occultation duration is normalized with respect to its diagonal. Two maximum slopes in each curve are associated with its length and its width. The slopes of the straight lines range between $1/\sqrt{2}$ (for square) and 1 (if length $\gg$ width).

4. Perspectives

Photometry of zipper mode data is something new that the TAOS project has developed. Synchronization of the data coming from all telescopes is one of the major features in this experiment. We are planning to apply the "rank statistics"[17,18] method to eliminate a statistical false positive. This way, a simultaneous dip in the data from all telescopes can be given a probability of detection and compared against the chance occurrence of a statistical fluctuation. We will need to compare the performance of this rank statistic algorithm against that of other photometric algorithms. With color information from other surveys available, we'll be able to estimate the distribution of target stars in a given field as a function of angular size. Currently, 500 to 720 nm band-pass filters are used for all telescopes. It is possible that we could obtain color information by using different filters. By considering the real spectrum of a distant star, it is also likely that we can have some calibration method for our system. Small comets are believed to be non-spherical in general. How a result derived from a spherical model can be extrapolated for a more general case is not clear at this time. Space-based experiments were proposed[14,26] for COROT and Kepler missions. The velocity of a satellite (typically, 7–8 km/s in some direction along its orbit) will contribute to the shadow speed in the shadow level. This alone might change the occultation event rate, which is proportional to the shadow speed, by 20–30%.

Acknowledgments

We thank Dr. Isao Sato (Nakano Star Gazers Club) and Dr. Kinoshita Daisuke for providing detail information on all the asteroid occultation predictions. KHC's was performed under the auspices of the U.S. Department of Energy, National Nuclear Security Administration by the University of California, Lawrence Livermore National Laboratory under contract No. W-7405-Eng-48.

References

1. K. E. Edgeworth, *Mon. Not. R. Astron. Soc.* **109**, 600 (1949).
2. G. P. Kuiper, in *Proceedings of a topical symposium, commemorating the 50th anniversary of the Yerkes Observatory and half a century of progress in astrophysics*, Ed. J. A. Hynek (McGraw-Hill, New York, 1951), p. 357.
3. D. Jewitt and J. Luu, *Nature* **362**, 730 (1993).
4. M. E. Brown, C. A. Trujillo and D. Rabinowitz, *IAUC* **8577** (2005).
5. M. E. Brown, C. A. Trujillo and D. Rabinowitz, *Astrophys. J.* **617**, 645 (2004).
6. G. M. Bernstein, D. E. Trilling, R. L. Allen, M. E. Brown, M. Holman and R. Malhotra, *Astron. J.* **128**, 1364 (2004).
7. S. J. Kenyon and B. C. Bromley, *Astron. J.* **128**, 1916 (2004).
8. M. E. Bailey, *Nature* **259**, 290 (1976).
9. M. J. Duncan and H. F. Levison, *Science* **276**, 1670 (1997).
10. K. H. Cook, C. Alcock, T. Axelrod and J. Lissauer, in *Bull. Am. Astron. Soc.* **27**, 1124 (1995).
11. S.-K. King, in *ASP Conf. Ser. 246: IAU Colloq. 183: Small Telescope Astronomy on Global Scales*, Ed. W.-P. Chen, C. Lemme and B. Paczyński (The Astronomical Society of the Pacific, San Francisco, 2001), p. 253.

12. C. Alcock, R. Dave, J. Giammarco *et al.*, *Earth Moon and Planets* **92**, 459 (2003).
13. F. Roques, M. Moncuquet and B. Sicardy, *Astron. J.* **93**, 1549 (1987).
14. F. Roques and M. Moncuquet, *Icarus* **147**, 530 (2000).
15. F. Roques, M. Moncuquet, N. Lavillonière, M. Auvergne, M. Chevreton, F. Colas and J. Lecacheux, *Astrophys. J.* **594**, L63 (2003).
16. A. Cooray, *Astrophys. J.* **589**, L97 (2003).
17. C. Liang, *The Detection of Stellar Occultation by Kuiper Belt Objects*, (PhD thesis, University of California, Berkeley, 2001).
18. C. Liang, J. A. Rice, I. de Pater, C. Alcock, T. Axelrod, A. Wang and S. Marshall, *Statistical Science* **19**, 265 (2004).
19. S. Marshall, C. Akerlof, R. Kehoe *et al.*, in *Bull. Am. Astron. Soc.* **29**, 1290 (1997).
20. R. C. Stone, S. W. McDonald and J. L. Elliot, *Astron. J.* **118**, 591 (1999).
21. D. V. Denissenko, *Astronomy Letters* **30**, 630 (2004).
22. W. P. Chen, Z. W. Zhang, S. K. King *et al.*, *Baltic Astronomy* **12**, 568 (2003).
23. O. Fors, J. Núñez and A. Richichi, *Astron. & Astrophys.* **378**, 1100 (2001).
24. O. Fors, E. P. Horch and J. Núñez, *Astron. & Astrophys.* **420**, 397 (2004).
25. M. J. I. Brown and R. L. Webster, *Mon. Not. R. Astron. Soc.* **289**, 783 (1997).
26. B. S. Gaudi, *Astrophys. J.* **610**, 1199 (2004).